IEEE Access
Multidisciplinary | Rapid Review | Open Access Journal

Received November 18, 2021, accepted December 14, 2021, date of publication December 16, 2021,
date of current version December 28, 2021.

Digital Object Identifier 10.1109/ACCESS.2021.3136249

Dynamical Analysis of a New Chaotic System: Hidden Attractor, Coexisting-Attractors, Offset Boosting, and DSP Realization

JUNJIE WEN[1], YIRAN FENG[1], XUEHENG TAO[2], AND YINGHONG CAO[2]
[1]School of Mechanical Engineering and Automation, Dalian Polytechnic University, Dalian 116034, China
[2]School of Information Science and Engineering, Dalian Polytechnic University, Dalian 116034, China

Corresponding authors: Yiran Feng (fengyr@dlpu.edu.cn) and Yinghong Cao (caoyinghong@dlpu.edu.cn)

This work was supported in part by the Dalian Young Stars of Science and Technology under Project 2021RQ088.

ABSTRACT In this paper, a new 5-D chaotic system with hidden attractor was presented. The stability and equilibrium points set of the system were analyzed by the traditional dynamical analysis method. Meanwhile, several special phenomena were found in the system, such as chaos degradation, state transition, multiwing chaotic attractors, coexisting-attractors etc. verifying the application of the system in engineering, offset boosting control method is introduced and numerical simulation of the system is implemented. In addition, the complexity of Spectral Entropy (SE) and C_0 are analyzed. Finally, the new system was simulated by the digital signal processing (DSP) technology, and the results agree well with the numerical simulation result. Theoretical analysis and simulation results show that the system has complex dynamical characteristics and can be applied to secure communication and image encryption.

INDEX TERMS Hidden attractor, coexisting-attractors, state transition, chaos degradation, offset boosting, DSP.

I. INTRODUCTION

The physical phenomenon that chaos is highly sensitive to initial value has attracted extensive attention. Since 1963, the famous Lorentz system [1] has been proposed, which clearly describes chaotic fundamental states sensitive to initial value conditions. So, in the last couple of decades, there's been a lot of interest from an engineering point of view in the creation of chaos. Chaotic systems [2]–[12] are widely used in information science, finance, biology, engineering and other fields. Up to now, a wide variety of chaotic systems have been studied, including hyperchaotic systems [13]–[16], multiwing chaotic systems [17]–[19], multiscroll chaotic systems [20]–[22], and chaotic systems with hidden attractor [23]–[27].

Especially chaotic systems with hidden attractor have become a hot topic in recent years. Such as Zhang *et al.* [28] revealed the local dynamical characteristics by studying two nonlinear systems with hidden attractor, and hidden attractor has many different characteristics from self-excited attractor due to its particularity. Thus, the particularity of the hidden attractor can be seen. At present, the academic definition of hidden attractor is that a basin of attraction of which does not contain neighborhoods of equilibria is called the hidden attractor. It usually exists in infinitely many equilibria chaotic system or non-equilibrium chaotic system. Meanwhile, the form of the hidden attractor can be periodic or chaotic attractor. Because of the special dynamical behavior of hidden attractor, the study of hidden attractor and the application of these nonlinear systems in engineering are of great physical significance and high project applicability. From the perspective of application, hidden oscillation will cause unnecessary losses to our production and life, so it is very important to understand this physical phenomenon to better grasp the chaotic motion and further lower the undesired behavior of chaos. In 2010, hidden attractors were first discovered in Chua circuits [29], [30] and hidden chaos attractors have been found in different systems. Therefore, Chen *et al.* [31] improved Chua circuit using memristor and analyzed its hidden attractor by numerical and experimental methods. Besides, in classical chaotic systems, such as Chen system [32]–[36], Lorenz system [37]–[39] and Lü system [40]–[42], scholars have also found the possibility of hidden attractor in these systems. Therefore,

The associate editor coordinating the review of this manuscript and approving it for publication was Stavros Souravlas.

Lai *et al.* [43] improved some classical chaotic systems, and found that coexisting-attractors and hidden attractor exist for some parameter regions. And Hu *et al.* [44] established the Sprott A system by combining two three-dimensional chaotic systems without equilibrium, which can generate multiscroll hidden attractor. It is found that chaotic systems with multi-scroll hidden attractors have greater complexity in nonlinear systems, and will have greater development prospects in the fields of image encryption and secure communication. In addition, multistability refers to the coexistence of two or more attractors with the same set of parameters under different initial values, and this is an interesting thing that usually happens in many nonlinear dynamical systems. It is well known that in a dynamical system, this phenomenon leads to very complex behaviors. In this paper, a new 5-D chaotic system is formed by modifying the 4D Yu-Wang chaotic system [45] Interestingly, the system has non-equilibrium, and it belongs to the category of chaotic systems with hidden attractor. Most of the existing non-equilibrium systems have very small constant parameters and a very small range of parameters to generate hidden chaotic attractors. So hidden attractors are hard to spot in these systems, and this system can easily generate hidden chaotic attractors whose constant terms can be very large. Meanwhile, the system also has complex dynamical phenomena, including multiwing chaotic attractors, state transition, chaos degradation, and coexisting-attractors [46]–[54]. Moreover, another very attractive feature of this system is the offset boosting [55]–[66], that means the system be able controlled flexibly by introducing a feedback state. Finally, the feasibility of the system is verified on DSP platform. The simple circuit structure of the system provides the possibility for the practical implementation of the circuit. Meanwhile, the complex dynamic behavior makes it have infinite practical application value, such as secure communication.

II. MATHEMATICAL MODEL

A. STABILITY AND EQUILIBRIUM POINTS SET

By introducing additional variable u and constant term k into the classical 4-D chaotic system, a new system is established as follows:

$$\begin{cases} \dot{x} = -ax + yz + bw + u \\ \dot{y} = cy - xz + k \\ \dot{z} = xy - dz \\ \dot{w} = xz - ew \\ \dot{u} = gy. \end{cases} \tag{1}$$

For the choice of initial state are (1, 1, 1, 1, 1), setting $a = 10$, $b = 2$, $c = 10$, $d = 21$, $k = 3$, $e = 10$, $g = 1.15$, The Lyapunov exponents spectrum calculated by MATLAB is as follows

$$\begin{aligned} &LE_1 = 2.3351, \quad \mathrm{LE}_2 = 0, \quad \mathrm{LE}_3 = -0.0254, \\ &LE_4 = -8.5586, \quad \mathrm{LE}_5 = -29.7577 \end{aligned} \tag{2}$$

Because the Lyapunov exponent in (2) is signed (+, 0, −, −, −), then the dynamic system (1) presents a chaotic state behavior. Kaplan-Yorke dimensions of the system (1) is found to be

$$D_{KY} = 4 + \frac{LE_1 + LE_2 + LE_3 + LE_4}{|LE_5|} = 3.79 \tag{3}$$

The conclusion of divergence of system (1) can be drawn

$$\Delta = \frac{\partial \dot{x}}{\partial x} + \frac{\partial \dot{y}}{\partial y} + \frac{\partial \dot{z}}{\partial z} + \frac{\partial \dot{w}}{\partial w} + \frac{\partial \dot{u}}{\partial u}, \tag{4}$$

setting $a = 10$, $b = 2$, $c = 10$, $d = 21$, $k = 3$, $e = 10$, $g = 1.15$ and the initial conditions are (1, 1, 1, 1, 1); then, $\Delta < 0$; therefore, the system is dissipative, and it can be inferred that the system has the possibility of chaotic attractors. Setting

$$\dot{x} = \dot{y} = \dot{z} = \dot{w} = \dot{u} = 0, \tag{5}$$

then

$$\begin{cases} -ax + yz + bw + u = 0 \\ cy - xz + k = 0 \\ xy - dz = 0 \\ xz - ew = 0 \\ gy = 0, \end{cases} \tag{6}$$

it is easy to get that

$$E = \begin{cases} None, & k = 0 \\ (n/a, 0, 0, 0, n), & k \neq 0, \end{cases} \tag{7}$$

When $k = 0$, let the equilibrium points set be O, Jacobi matrix J_E of the system (1) set is

$$J_E = \begin{bmatrix} -a & z & y & b & 1 \\ -z & c & -x & 0 & 0 \\ y & x & -d & 0 & 0 \\ z & 0 & x & -e & 0 \\ 0 & g & 0 & 0 & 0 \end{bmatrix},$$

and the characteristic equation for the equilibrium points O

$$\lambda^5 + a_1\lambda^4 + a_2\lambda^3 + a_3\lambda^2 + a_4\lambda + a_5 = 0, \tag{8}$$

where $a_1 = 31$, $a_2 = 109$, $a_3 = -3069.85$, $a_4 = -20093.2$, $a_5 = 253$.

According to Eq. (4), the system is unstable if the coefficient of the characteristic equation has negative coefficient terms. Therefore, Let n be an arbitrary constant, and any equilibrium points within O $(n/a, 0, 0, 0, n)$, when parameters are $n = 10$, $a = 10$, $b = 2$, $c = 10$, $d = 21$, $k = 3$, $e = 10$, and $g = 1.15$, we can obtain $a_3 = -3069.85 < 0$, $a_4 = -20093.2 < 0$, and $\lambda_1 = 9.9075$, $\lambda_2 = -21.0482$, $\lambda_3 = --11.4137$, $\lambda_4 = -8.4582$, $\lambda_5 = 0.0126$. This means that the system is unstable and can create chaos.

III. NUMERICAL DIAGRAM OF THE DYNAMICAL BEHAVIORS

A. HIDDEN CHAOTIC ATTRACTOR

A basin of attraction of which does not contain neighborhoods of equilibria is called the hidden attractor. When there is no equilibrium point or infinite equilibrium point in

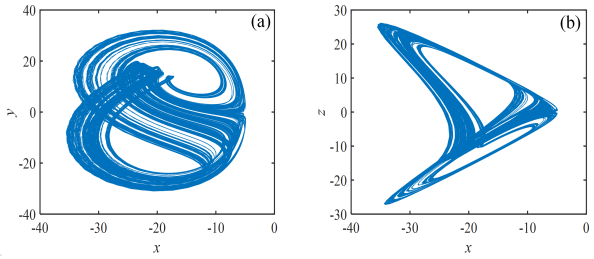

FIGURE 1. Hidden chaotic attractor: (a) *X-Y* plane and (b) *X-Z* plane.

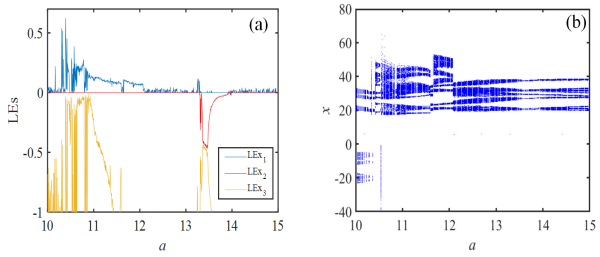

FIGURE 2. (a) Lyapunov exponent spectrum and (b) bifurcation diagram.

the chaotic system equation, the chaotic attractor is hidden chaotic attractor. Set $a = 10$, $b = 2$, $c = 10$, $d = 21$, $k = 3$, $e = 10$, and $g = 1.15$, and initial condition (1, 1, 1, 1, 1). Since $k \neq 0$ there is no equilibrium. Therefore, the chaotic attractor is the hidden chaotic attractor. As shown in Fig.1, the phase diagrams of different phase planes of hidden chaotic attractors in the system are given.

B. LYAPUNOV EXPONENTIAL SPECTRUM AND BIFURCATION DIAGRAM OF THE SYSTEM

Three variable system parameters are determined by system (1) as a, e and d. The parameter region of interest is specified as $a \in [10, 15]$, $e \in [10, 30]$, and $d \in [20, 35]$.

By combining the bifurcation diagram with Lyapunov exponential spectrum, its states under different parameters can be obtained. Parameters a, e and d, were taken as variables, the initial value are (1, 1, 1, 1, 1), the step is $h = 0.01$s, the remaining parameters of the equation were fixed, and different states of the chaotic system can be observed by changing parameters a, e and d.

Take the parameter $a \in [10, 15]$, and let $b = 2$, $c = 10$, $d = 21$, $k = 3$, $e = 10$, and $g = 1.15$. The Lyapunov exponential spectrum and bifurcation diagram are shown in Fig.2. For the sake of observation, the smaller LEs are omitted below. With the change of parameter a, complex dynamical characteristics such as chaos and period appear successively in the system. At the same time, an interesting phenomenon is found in the bifurcation diagram, which shows that the multiwing chaos transforms into chaos. In Fig.3, with different parameter a, it represents the attractors of the system in three different states including multiwing chaos attractors, chaos attractors, quasi-periodic attractors. In addition, refer to Table 1. It can clearly understand the change of system state when parameter a changes.

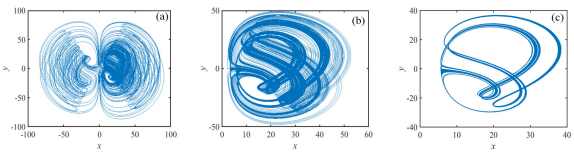

FIGURE 3. Different states with $b = 2$, $c = 10$, $d = 21$, $k = 3$, $e = 10$, and $g = 1.15$: (a) multiwing chaos for $a = 10.45$, (b) chaos for $a = 11.5$, and (c) period for $a = 12.47$.

TABLE 1. Corresponding state and LEs with the initial conditions (1, 1, 1, 1, 1), the parameters $b = 2$, $c = 10$, $d = 21$, $k = 3$, $e = 10$, $g = 1.15$, and the different parameter a.

Range	LEs	State	Range	LEs	State
	0 - - - -	Divergence	12.49-12.51	0 - - - -	Period
10-10.34	+ 0 - - -	Multiwing-chaos	12.52-12.67	+ 0 - - -	Chaos
10.35-10.49	+ 0 - - -	Chaos	12.68-12.7	+ 0 - - -	Weak chaos
10.5	0 - - - -	Period	12.71-12.81	+ 0 - - -	Chaos
10.51-10.79	+ 0 - - -	Weak chaos	12.82-12.87	0 - - - -	Period
10.8	0 - - - -	Period	12.88-13.06	+ 0 - - -	Chaos
10.81-11.64	+ 0 - - -	Chaos	13.07-13.12	0 - - - -	Period
11.65	+ 0 - - -	Weak chaos	13.12-13.17	+ 0 - - -	Weak chaos
11.66-12.09	+ 0 - - -	Chaos	13.18-13.22	0 - - - -	Period
12.10-12.12	+ 0 - - -	Weak chaos	13.23-13.32	+ 0 - - -	Weak chaos
12.13-12.22	+ 0 - - -	Chaos	13.33-13.45	0 - - - -	Period
12.23-12.24	0 - - - -	Period	13.46-13.58	+ 0 - - -	Weak chaos
12.25-12.28	+ 0 - - -	Chaos	13.59-13.9	0 - - - -	Period
12.29-12.30	0 - - - -	Period	13.91-15	+ 0 - - -	Weak chaos
12.31-12.48	+ 0 - - -	Chaos	13.91-15	+ 0 - - -	Weak chaos

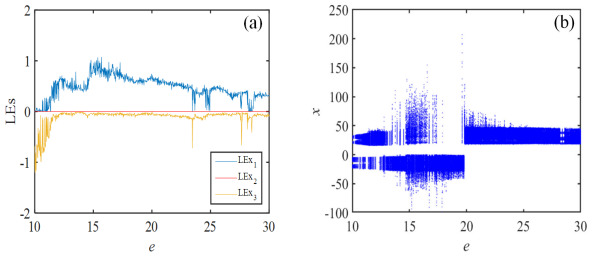

FIGURE 4. (a) Lyapunov exponent spectrum and (b) bifurcation diagram.

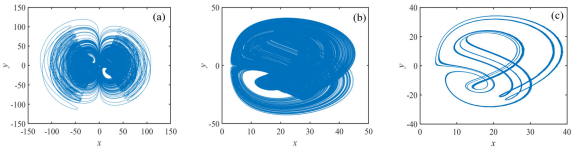

FIGURE 5. Different states with $a = 10$, $b = 2$, $c = 10$, $d = 21$, $k = 3$, and $g = 1.15$: (a) multiwing chaos for $e = 16$, (b) chaos for $e = 25$, and (c) period for $e = 28.5$.

Take the parameter $e \in [10, 30]$ and leave the other parameters unchanged. It can be observed from Fig.4 when $e \in [10, 19.8]$, the system is in a chaotic state accompanied by multiwing. And when $e \in [28.15, 28.55]$, it is found that the system changes from chaos to periodicity, indicating that the system has complex dynamical characteristics. The phase diagram of the system in different states is shown in Figure 5. As shown in Table 2, when parameter e is at different values, states of the system presented are greatly different.

Take the parameter $d \in [20, 35]$, and keep the other parameters fixed. In Fig.6, when parameter $d = 25.7$, the maximum LEs value is 2.66, indicating that the system has very complex dynamical characteristics and has a very good application prospect in encrypted communication. Meanwhile, in Fig. 7,

TABLE 2. Corresponding state and LEs with the initial conditions (1, 1, 1, 1, 1), the parameters $a = 10$, $b = 2$, $c = 10$, $d = 21$, $k = 3$, $g = 1.15$ and the different parameter e.

Range	LEs	State	Range	LEs	State
	0 - - - -	Divergence	11.35-28.24	+ 0 - - -	Multiwing-chaos
10-11.06	+ 0 - - -	Weak chaos	28.25-28.6	0 - - - -	Period
11.07-11.33	+ 0 - - -	Chaos	28.61-30	+ 0 - - -	Chaos
11.34	0 - - - -	Period			

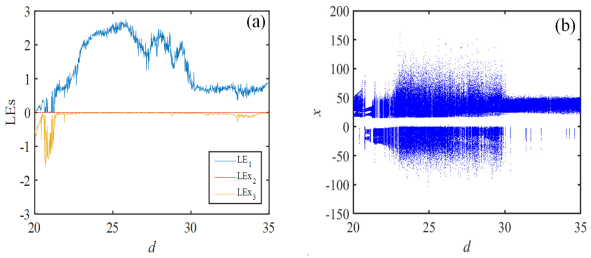

FIGURE 6. (a) Lyapunov exponent spectrum and (b) bifurcation diagram.

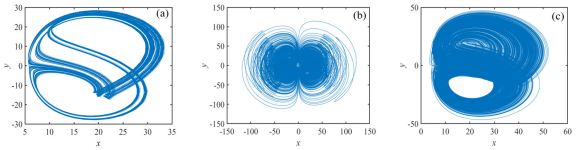

FIGURE 7. Different states with $a = 10$, $b = 2$, $c = 10$, $k = 3$, $e = 10$, and $g = 1.15$: (a) multiwing chaos for $d = 21$, (b) chaos for $d = 25$, and (c) period for $d = 32$.

TABLE 3. Corresponding state and LEs with the initial conditions (1, 1, 1, 1, 1), the parameters $a = 10$, $b = 2$, $c = 10$, $e = 10$, $k = 3$, $g = 1.15$, and the different parameter d.

Range	LEs	State	Range	LEs	State
	0 - - - -	Divergence	20.64-21.06	0 - - - -	Period
20-20.36	+ 0 - - -	Chaos	21.07-21.26	+ 0 - - -	Weak chaos
20.37	+ 0 - - -	Weak chaos	21.27-28.5	+ 0 - - -	Multiwing-chaos
20.38-20.63	+ 0 - - -	Chaos	28.5-35	+ 0 - - -	Chaos

phase diagrams in different states are shown along with different parameter d. According to Table 3, we can clearly understand how the change of parameter e affects the change of dynamical characteristics of the system.

C. CHAOS DEGRADATION AND STATE TRANSITION

The state of the system is sometimes instable, and when the system leaves different dynamical regions, the system will show rich dynamical characteristics. Set $a = 10$, $b = 2$, $c = 10$, $d = 21$, $k = 3$, $e = 28.15$, and $g = 1.15$, set the simulation step size as 0.01s, select the initial value as (1, 1, 1, 1, 1). It can be observed that the dynamical system appears the phenomenon of state transition. As shown in Fig.8, the dynamical system has experienced the phenomenon from chaos to periodic and then to chaos. As can be seen in Fig.9 at $t \in [0, 250]$, the system is in a chaotic state. As can be seen in Fig.10, at $t \in [300, 1000]$, the system is in a periodic state.

Sometimes chaos degradation also occurs in this dynamical system. As shown in Fig.11, it is obvious that the system

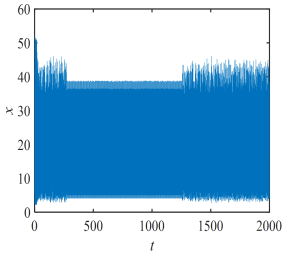

FIGURE 8. Time-domain waveform.

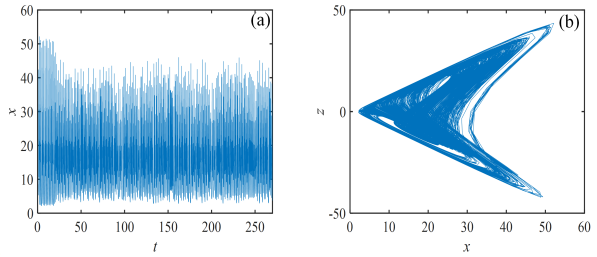

FIGURE 9. (a) Time-domain waveform and (b) phase diagram.

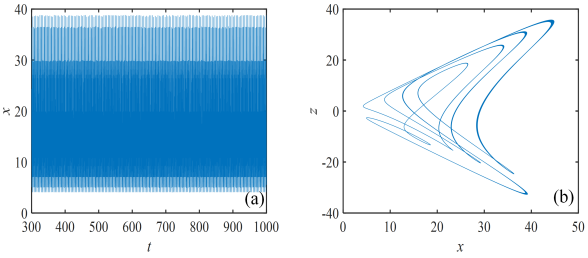

FIGURE 10. (a) Time-domain waveform and (b) phase diagram.

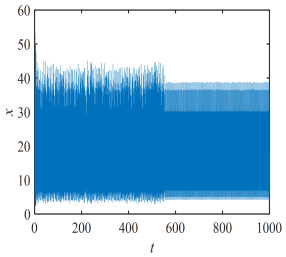

FIGURE 11. Time-domain waveform.

degenerates from chaos to period. As shown in Fig.12, at $t \in [0, 500]$, chaos appears in the system. As shown in Fig.13, at $t \in [600, 1000]$, the system is in a periodic state.

D. COEXISTING-ATTRACTORS

Coexisting-attractor is special phenomenon that occurs mainly in some special nonlinear systems and has become hot research feature. When parameters are constant and the initial value is changed, the system orbit may trend to different motion states. Suppose $a = 11$, $b = 2$, $c = 10$, $d = 21$, $k = 3$, $e = 10$, and $g = 1.15$, step size is 0.01, set the initial values as (1, 1, 1, 1, 1) and $(-1, -1, -1, -1, -0.01)$ respectively, and the symmetrical attractor phenomenon as shown in Fig.14 can

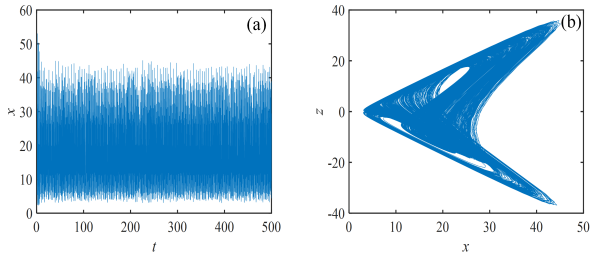

FIGURE 12. (a) Time-domain waveform and (b) phase diagram.

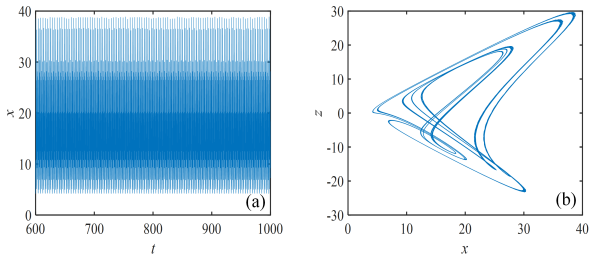

FIGURE 13. (a) Time-domain waveform and (b) phase diagram.

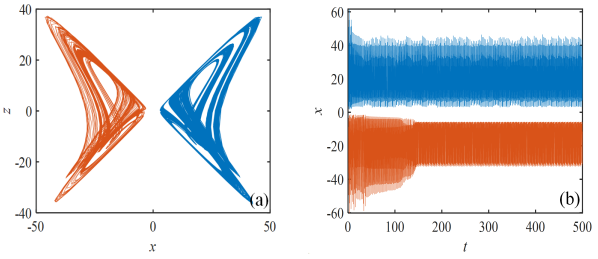

FIGURE 14. (a) Attractors in x–z plane and (b) time-domain waveform.

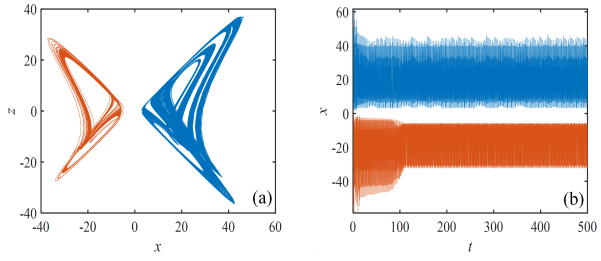

FIGURE 15. (a) Attractors in x–z plane and (b) time-domain waveform.

be observed. Set the initial values are set as (1, 1, 1, 1, 1) and (−2, −2, −2, −2, −0.01), the phenomenon of asymmetrical coexisting-attractors can be observed as shown in Fig.15. In Fig 16, the location of initial values in different color regions can produce different types of state attractors. It shows that the system has many kinds of coexisting attractors. The rich changes of different colors in the figure prove that the system has rich asymmetric multi-steady states. At the same time, we also implemented the coexistence attractor on circuit, as shown in Figure 17.

E. OFFSET BOOSTING SCHEME

Offset boosting is a method of moving the system's attractors and its basin of attractors arbitrarily without changing the

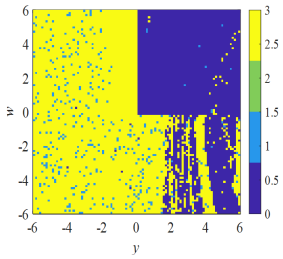

FIGURE 16. Basins of coexisting attractions.

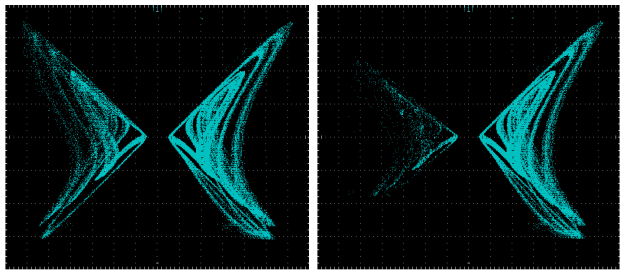

FIGURE 17. Circuit implementation of coexisting attractors.

system solution. This means that with the introduction of feedback states, the system can be flexibly controlled. Since the state variable w appears only once in the system equation as a linear term, Therefore, the boosting of variable u can be controlled by parameter q. The improved system based on System (2) is as follows:

$$\begin{cases} \dot{x} = -ax + yz + bw + (u - q) \\ \dot{y} = cy - xz + k \\ \dot{z} = xy - dz \\ \dot{w} = xz - ew \\ \dot{u} = gy, \end{cases} \tag{9}$$

where q is a constant. Setting $a = 11$, $b = 2$, $c = 10$, $d = 21$, $k = 3$, $e = 10$, $g = 1.15$, and the 3-D projections of attractors with different offsets q are shown Fig.16(a). In the Fig.16(b) with the parameter q increases, the bifurcation diagram shows a regular upward trend. The Lyapunov exponential spectrum and bifurcation diagram are shown in Fig.17(a) and Fig.17(b). Here, for the sake of observation, the smaller Les are omitted in Lyapunov exponent spectrums. When the parameter $q \in [60, 70]$, it can be found that the system state variable w increases with the increase of offset q. Meanwhile, the Lyapunov exponential spectrum in Fig.17 (b) remains unchanged, indicating that the state of the system does not change with the offset q. In a word, this method can make the attractor shift in a certain direction flexibly by introducing the offset, which has great engineering application value.

F. COMPLEXITY ANALYSIS

The complexity of nonlinear system systems has become a hot topic research. The approximation of chaotic sequence and random sequence is measured by complexity algorithm. Fig 18 shows the complexity diagrams of different a and d

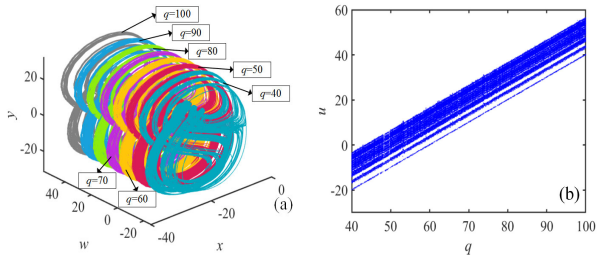

FIGURE 18. (a) Attractors with different offset q and (b) bifurcation diagram with offset q.

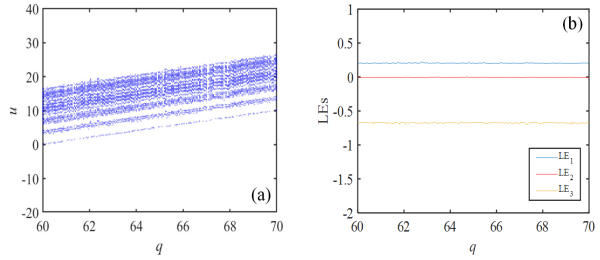

FIGURE 19. (a) Bifurcation diagram with offset q and (b) Lyapunov exponent spectrum with offset q.

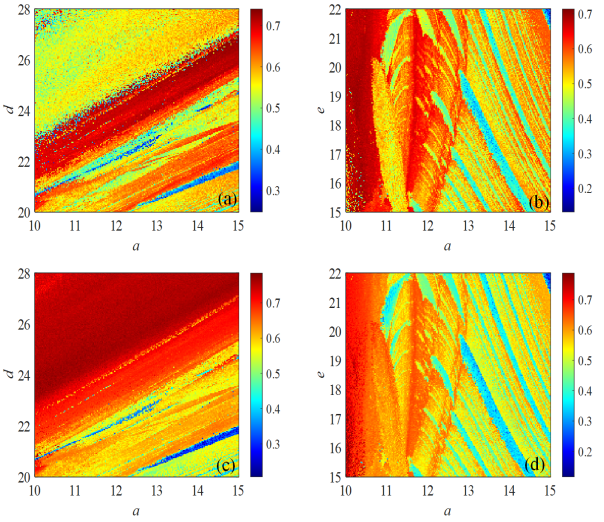

FIGURE 20. (a) SE complexity parameters of the a d. (b) SE complexity parameters of the a e. (c) C_0 complexity parameters of the a d. (d) C_0 complexity parameters of the a e.

as well as a and e to analyze the complexity of the nonlinear system. In Fig.18 (c), when $a \in [10, 15]$ and $d \in [23, 28]$, it can be seen that this area is red, meaning that the system is in chaos. Hence, the darker the color in the figure, the higher the complexity of the chaotic system under the corresponding parameters, and the method of complexity analysis provides a reliable basis for parameter selection of multivariable complex chaotic graph system.

IV. DSP IMPLEMENTATION

DSP chip F28335 has high efficiency and little influence on the environment. Therefore, it is an ideal platform for verifying new 5-D chaotic systems. The DSP-controlled D/A commutator needs to commutate the DSP-generated sequence code simulation to better catch the oscilloscope, and the output sequence is represented on the oscillation range.

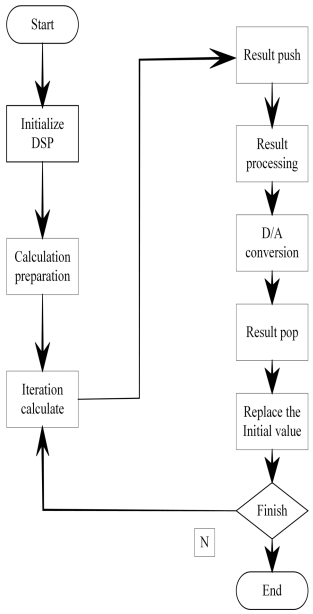

FIGURE 21. Programming flow of DSP implementation.

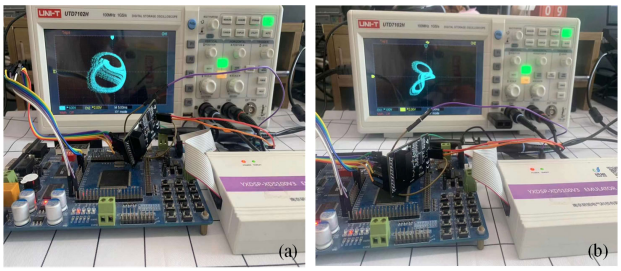

FIGURE 22. Experimental platform for DSP implementation.

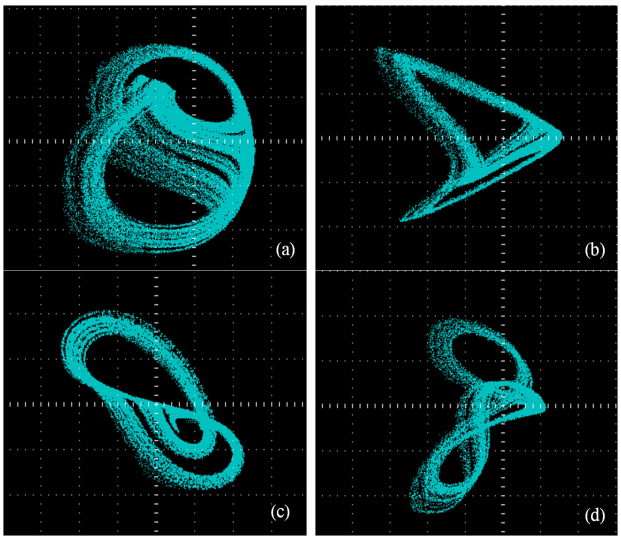

FIGURE 23. Chaotic attractor implemented on DSP platform: (a) X-Y plane, (b) X-Z plane, (c) Y-Z plane, and (d) X-W plane.

In terms of software design, in order to make the equipment only suitable for processing discrete system can process the new 5-D chaotic system on the DSP platform, the continuous nonlinear system needs to be discretized first. So, the continuous nonlinear system is discretized and transformed into discrete chaotic sequence. Then C language is used to write the reduplicative relation into DSP board. The programming process and experimental platform are shown in Fig 19.

Setting the parameters as $a = 10$, $b = 2$, $c = 10$, $d = 21$, $k = 3$, $e = 10$, and $g = 1.15$, the initial conditions are (1, 1, 1, 1, 1), the experimental platform is shown in Fig.20, which is one-to-one corresponding to Fig.1 (a) and (d). It can be seen from Fig.21 that the four phase diagrams obtained are exactly the same as those in Fig.1, which proves the correctness of the digital circuit simulation of the system.

V. CONCLUSION

In this paper, a new 5-D chaotic system is presented and its dynamical behavior is studied numerically. It is shown that chaotic systems with hidden attractors have very complex dynamical. Firstly, the system has a variety of attractors, including chaotic attractors, periodic attractors, and multi-wing chaotic attractors. Another obvious feature is that the system has a variety of different types of coexistence attractors. Meantime, when the parameters change, the system appears chaos degradation and state transition, which means that the system has very rich dynamic behavior. In order to realize the offset boosting control, control variable q is introduced into state variable u. The state variable u varies linearly with offset q, and the value of LEs is found to have little change, indicating that the u sequence can be flexibly changed by introducing control variables. Finally, the system is implemented on DSP platform, and experiments are carried out on DSP platform to verify the consistency of experimental results and numerical analysis results. References are provided in this paper for the study of hidden chaotic attractors, the offset boosting control and circuit experiments.

REFERENCES

[1] E. N. Lorenz, "Deterministic nonperiodic flow," *J. Atmos. Sci.*, vol. 20, no. 2, pp. 130–141, 1963.

[2] Y. Peng, K. Sun, and S. He, "A discrete memristor model and its application in Hénon map," *Chaos, Solitons Fractals*, vol. 137, Aug. 2020, Art. no. 109873.

[3] Y.-X. Peng, K.-H. Sun, and S.-B. He, "Dynamics analysis of chaotic maps: From perspective on parameter estimation by meta-heuristic algorithm," *Chin. Phys. B*, vol. 29, no. 3, Mar. 2020, Art. no. 030502.

[4] X. Ma, J. Mou, J. Liu, C. Ma, F. Yang, and X. Zhao, "A novel simple chaotic circuit based on memristor–memcapacitor," *Nonlinear Dyn.*, vol. 100, no. 3, pp. 2859–2876, May 2020.

[5] X. Han, J. Mou, L. Xiong, C. Ma, T. Liu, and Y. Cao, "Coexistence of infinite attractors in a fractional-order chaotic system with two nonlinear functions and its DSP implementation," *Integration*, vol. 81, pp. 43–55, Nov. 2021.

[6] C. Ma, J. Mou, P. Li, F. Yang, and T. Liu, "Multistability analysis and digital circuit implementation of a new conformable fractional-order chaotic system," *Mobile Netw. Appl.*, vol. 6, pp. 1–10, Jul. 2020.

[7] S. Qiao and X.-L. An, "Dynamic expression of a HR neuron model under an electric field," *Int. J. Modern Phys. B*, vol. 35, no. 2, Jan. 2021, Art. no. 2150024.

[8] Y. Peng, S. He, and K. Sun, "A higher dimensional chaotic map with discrete memristor," *AEU Int. J. Electron. Commun.*, vol. 129, Feb. 2021, Art. no. 153539.

[9] Y. Peng, S. He, and K. Sun, "Chaos in the discrete memristor-based system with fractional-order difference," *Results Phys.*, vol. 24, May 2021, Art. no. 104106.

[10] F. Yang, J. Mou, C. Ma, and Y. Cao, "Dynamic analysis of an improper fractional-order laser chaotic system and its image encryption application," *Opt. Lasers Eng.*, vol. 129, Jun. 2020, Art. no. 106031.

[11] X. Li, J. Mou, L. Xiong, Z. Wang, and J. Xu, "Fractional-order double-ring erbium-doped fiber laser chaotic system and its application on image encryption," *Opt. Laser Technol.*, vol. 140, Aug. 2021, Art. no. 107074.

[12] T. Liu, S. Banerjee, H. Yan, and J. Mou, "Dynamical analysis of the improper fractional-order 2D-SCLMM and its DSP implementation," *Eur. Phys. J. Plus*, vol. 136, no. 5, pp. 1–17, 2021.

[13] Z. Chen, H. Zhao, and J. Chen, "A novel image encryption scheme based on poker cross-shuffling and fractional order hyperchaotic system," in *Proc. Int. Conf. Comput. Eng. Netw.*, vol. 1274. Singapore: Springer, 2020, pp. 818–825.

[14] S. F. Al-Azzawi and A. S. Al-Obeidi, "Chaos synchronization in a new 6D hyperchaotic system with self-excited attractors and seventeen terms," *Asian-Eur. J. Math.*, vol. 14, no. 5, May 2021, Art. no. 2150085.

[15] F. Yu, L. Li, B. He, L. Liu, S. Qian, Z. Zhang, H. Shen, S. Cai, and Y. Li, "Pseudorandom number generator based on a 5D hyperchaotic four-wing memristive system and its FPGA implementation," *Eur. Phys. J. Special Topics*, vol. 230, pp. 1763–1772, Jun. 2021.

[16] X. Chen, S. Qian, F. Yu, Z. Zhang, H. Shen, Y. Huang, S. Cai, Z. Deng, Y. Li, and S. Du, "Pseudorandom number generator based on three kinds of four-wing memristive hyperchaotic system and its application in image encryption," *Complexity*, vol. 2020, pp. 1–17, Dec. 2020.

[17] X. Zhong, M. Peng, and M. Shahidehpour, "Creation and circuit implementation of two-to-eight-wing chaotic attractors using a 3D memristor-based system," *Int. J. Circuit Theory Appl.*, vol. 47, no. 5, pp. 686–701, 2019.

[18] L. Cui, M. Lu, Q. Ou, H. Duan, and W. Luo, "Analysis and circuit implementation of fractional order multi-wing hidden attractors," *Chaos, Solitons Fractals*, vol. 138, Sep. 2020, Art. no. 109894.

[19] Q. Deng, C. Wang, and L. Yang, "Four-wing hidden attractors with one stable equilibrium point," *Int. J. Bifurcation Chaos*, vol. 30, no. 6, May 2020, Art. no. 2050086.

[20] D. Mathale, E. F. D. Goufo, and M. Khumalo, "Coexistence of multi-scroll chaotic attractors for fractional systems with exponential law and non-singular kernel," *Chaos, Solitons Fractals*, vol. 139, Oct. 2020, Art. no. 110021.

[21] Y. Wu, C. Wang, and Q. Deng, "A new 3D multi-scroll chaotic system generated with three types of hidden attractors," *Eur. Phys. J. Spec. Top.*, vol. 230, pp. 1863–1871, 2021.

[22] H. Lu, K. Rajagopal, F. Nazarimehr, and S. Jafari, "A new multi-scroll megastable oscillator based on the sign function," *Int. J. Bifurcation Chaos*, vol. 31, no. 8, Jun. 2021, Art. no. 2150140.

[23] M. Ji'e, D. Yan, L. Wang, and S. Duan, "Hidden attractor and multistability in a novel memristor-based system without symmetry," *Int. J. Bifurcation Chaos*, vol. 31, no. 11, Sep. 2021, Art. no. 2150168.

[24] J. R. Pulido-Luna, J. A. López-Rentería, N. R. Cazarez-Castro, and E. Campos, "A two-directional grid multiscroll hidden attractor based on piecewise linear system and its application in pseudo-random bit generator," *Integration*, vol. 81, pp. 34–42, Jun. 2021.

[25] C. Ma, J. Mou, L. Xiong, S. Banerjee, T. Liu, and X. Han, "Dynamical analysis of a new chaotic system: Asymmetric multistability, offset boosting control and circuit realization," *Nonlinear Dyn.*, vol. 103, no. 3, pp. 2867–2880, 2021.

[26] X. An and S. Qiao, "The hidden, period-adding, mixed-mode oscillations and control in a HR neuron under electromagnetic induction," *Chaos, Solitons Fractals*, vol. 143, Feb. 2021, Art. no. 110587.

[27] T. Liu, H. Yan, S. Banerjee, and J. Mou, "A fractional-order chaotic system with hidden attractor and self-excited attractor and its DSP implementation," *Chaos, Solitons Fractals*, vol. 145, Apr. 2021, Art. no. 110791.

[28] G. Zhang, F. Wu, C. Wang, and J. Ma, "Synchronization behaviors of coupled systems composed of hidden attractors," *Int. J. Modern Phys. B*, vol. 31, no. 26, Oct. 2017, Art. no. 1750180.

[29] Y. Fei, S. A. Hui, A. Zz, A. Yh, A. Sc, and C. Sd, "A new multi-scroll Chua's circuit with composite hyperbolic tangent-cubic nonlinearity: Complex dynamics, hardware implementation and image encryption application," *Integration*, vol. 81, pp. 71–83, Jun. 2021.
[30] A. I. Ahamed and M. Lakshmanan, "Sliding bifurcations in the memristive Murali–Lakshmanan–Chua circuit and the memristive driven Chua oscillator," *Int. J. Bifurcation Chaos*, vol. 30, no. 14, Nov. 2020, Art. no. 2050214.
[31] M. Chen, M. Li, Q. Yu, B. Bao, Q. Xu, and J. Wang, "Dynamics of self-excited attractors and hidden attractors in generalized memristor-based Chua's circuit," *Nonlinear Dyn.*, vol. 81, nos. 1–2, pp. 215–226, 2015.
[32] B. Wang, L. Li, and Y. Wang, "An efficient nonstandard finite difference scheme for chaotic fractional-order Chen system," *IEEE Access*, vol. 8, pp. 98410–98421, 2020.
[33] M. Suqi, "Two-dimensional manifolds of modified Chen system with time delay," *Int. J. Bifurcation Chaos*, vol. 31, no. 9, Jul. 2021, Art. no. 2150174.
[34] H. P. Ren, K. Tian, and C. Grebogi, "Topological horseshoe in a single-scroll Chen system with time delay," *Chaos, Solitons Fractals*, vol. 132, Mar. 2020, Art. no. 109593.
[35] J. Cermák and L. Nechvátal, "Stability and chaos in the fractional Chen system," *Chaos, Solitons Fractals*, vol. 125, pp. 24–33, Aug. 2019.
[36] C. Yin, "Chaos detection of the Chen system with Caputo–Hadamard fractional derivative," *Int. J. Bifurcation Chaos*, vol. 31, no. 1, Jan. 2021, Art. no. 2150016.
[37] J. N. Kouagou, P. G. Dlamini, and S. M. Simelane, "On the multi-domain compact finite difference relaxation method for high dimensional chaos: The nine-dimensional Lorenz system," *Alexandria Eng. J.*, vol. 59, no. 4, pp. 2617–2625, 2020.
[38] S. Tariq, M. Khan, A. Alghafis, and M. Amin, "A novel hybrid encryption scheme based on chaotic Lorenz system and logarithmic key generation," *Multimedia Tools Appl.*, vol. 79, no. 31, pp. 23507–23529, 2020.
[39] C. Zou, Q. Zhang, X. Wei, and C. Liu, "Image encryption based on improved Lorenz system," *IEEE Access*, vol. 8, pp. 75728–75740, 2020.
[40] J. Guo, C. Ma, Z. Wang, and F. Zhang, "Time-delay characteristics of complex lü system and its application in speech communication," *Entropy*, vol. 22, no. 11, p. 1260, Nov. 2020.
[41] B. Yan, S. He, and S. Wang, "Multistability and formation of spiral waves in a fractional-order memristor-based hyperchaotic lü system with no equilibrium points," *Math. Problems Eng.*, vol. 2020, p. 12, Jun. 2020.
[42] H. Jia, W. Shi, and G. Qi, "Coexisting attractors, energy analysis and boundary of lü system," *Int. J. Bifurcation Chaos*, vol. 30, no. 3, Mar. 2020, Art. no. 2050048.
[43] Q. Lai, Z. Wan, and P. D. Kamdem Kuate, "Modelling and circuit realisation of a new no-equilibrium chaotic system with hidden attractor and coexisting attractors," *Electron. Lett.*, vol. 56, no. 20, pp. 1044–1046, Sep. 2020.
[44] X. Hu, C. Liu, L. Liu, J. Ni, and S. Li, "Multi-scroll hidden attractors in improved sprott a system," *Nonlinear Dyn.*, vol. 86, no. 3, pp. 1725–1734, Nov. 2016.
[45] F. Yu, L. Liu, H. Shen, Z. Zhang, Y. Huang, S. Cai, Z. Deng, and Q. Wan, "Multistability analysis, coexisting multiple attractors, and FPGA implementation of Yu–Wang Four-Wing chaotic system," *Math. Problems Eng.*, vol. 2020, pp. 1–16, Aug. 2020.
[46] N. Debbouche, A. O. Almatroud, A. Ouannas, and I. M. Batiha, "Chaos and coexisting attractors in glucose-insulin regulatory system with incommensurate fractional-order derivatives," *Chaos, Solitons Fractals*, vol. 143, Feb. 2021, Art. no. 110575.
[47] J. Cui and B.-W. Shen, "A kernel principal component analysis of coexisting attractors within a generalized Lorenz model," *Chaos, Solitons Fractals*, vol. 146, May 2021, Art. no. 110865.
[48] N. Saeed, S. Çiçek, A. C. Chamgoué, S. T. Kingni, and Z. Wei, "Bistable and coexisting attractors in current modulated edge emitting semiconductor laser: Control and microcontroller-based design," *Opt. Quantum Electron.*, vol. 53, no. 6, pp. 1–12, Jun. 2021.
[49] K. Rajagopal, H. Jahanshahi, S. Jafari, R. Weldegiorgis, A. Karthikeyan, and P. Duraisamy, "Coexisting attractors in a fractional order hydro turbine governing system and fuzzy PID based chaos control," *Asian J. Control*, vol. 23, no. 2, pp. 894–907, Mar. 2021.
[50] S. Fu and Y. Liu, "Complex dynamical behavior of modified MLC circuit," *Chaos, Solitons Fractals*, vol. 141, Dec. 2020, Art. no. 110407.
[51] C. Ma, J. Mou, P. Li, and T. Liu, "Dynamic analysis of a new two-dimensional map in three forms: Integer-order, fractional-order and improper fractional-order," *Eur. Phys. J. Special Topics*, vol. 230, nos. 7–8, pp. 1945–1957, Aug. 2021.
[52] Q. Lai, "A unified chaotic system with various coexisting attractors," *Int. J. Bifurcation Chaos*, vol. 31, no. 1, Jan. 2021, Art. no. 2150013.
[53] Q. Lai, B. Norouzi, and F. Liu, "Dynamic analysis, circuit realization, control design and image encryption application of an extended lü system with coexisting attractors," *Chaos, Solitons Fractals*, vol. 114, pp. 230–245, Sep. 2018.
[54] Q. Lai, Z. Wan, L. K. Kengne, P. D. K. Kuate, and C. Chen, "Two-memristor-based chaotic system with infinite coexisting attractors," *IEEE Trans. Circuits Syst. II, Exp. Briefs*, vol. 68, no. 6, pp. 2197–2201, Jun. 2021.
[55] S. T. Kingni, K. Rajagopal, S. Çiçek, A. Srinivasan, and A. Karthikeyan, "Dynamic analysis, FPGA implementation, and cryptographic application of an autonomous 5D chaotic system with offset boosting," *Frontiers Inf. Technol. Electron. Eng.*, vol. 21, no. 6, pp. 950–961, Jun. 2020.
[56] H. Bao, W. Liu, J. Ma, and H. Wu, "Memristor initial-offset boosting in memristive HR neuron model with hidden firing patterns," *Int. J. Bifurcation Chaos*, vol. 30, no. 10, Aug. 2020, Art. no. 2030029.
[57] Y. Yang, K. Ren, H. Qian, and X. Yao, "A simple hyperchaotic circuit with coexisting multiple bifurcations and offset boosting," *Eur. Phys. J. Special Topics*, vol. 229, nos. 6–7, pp. 1163–1174, Mar. 2020.
[58] S. Gu, S. He, H. Wang, and B. Du, "Analysis of three types of initial offset-boosting behavior for a new fractional-order dynamical system," *Chaos, Solitons Fractals*, vol. 143, Feb. 2021, Art. no. 110613.
[59] H. Wu, Y. Ye, B. Bao, M. Chen, and Q. Xu, "Memristor initial boosting behaviors in a two-memristor-based hyperchaotic system," *Chaos, Solitons Fractals*, vol. 121, pp. 178–185, Apr. 2019.
[60] A. Sambas, S. Vaidyanathan, E. Tlelo-Cuautle, B. Abd-El-Atty, A. A. A. El-Latif, O. Guille-Fernandez, Sukono, Y. Hidayat, and G. Gundara, "A 3-D multi-stable system with a peanut-shaped equilibrium curve: Circuit design, FPGA realization, and an application to image encryption," *IEEE Access*, vol. 8, pp. 137116–137132, 2020.
[61] G. Peng and F. Min, "Multistability analysis, circuit implementations and application in image encryption of a novel memristive chaotic circuit," *Nonlinear Dyn.*, vol. 90, no. 3, pp. 1607–1625, Nov. 2017.
[62] A. Sambas, S. Vaidyanathan, S. Zhang, Y. Zeng, M. A. Mohamed, and M. Mamat, "A new double-wing chaotic system with coexisting attractors and line equilibrium: Bifurcation analysis and electronic circuit simulation," *IEEE Access*, vol. 7, pp. 115454–115462, 2019.
[63] S. Mobayen, A. Fekih, S. Vaidyanathan, and A. Sambas, "Chameleon chaotic systems with quadratic nonlinearities: An adaptive finite-time sliding mode control approach and circuit simulation," *IEEE Access*, vol. 9, pp. 64558–64573, 2021.
[64] A. Sambas, S. Vaidyanathan, T. Bonny, S. Zhang, Sukono, Y. Hidayat, G. Gundara, and M. Mamat, "Mathematical model and FPGA realization of a multi-stable chaotic dynamical system with a closed butterfly-like curve of equilibrium points," *Appl. Sci.*, vol. 11, no. 2, p. 788, Jan. 2021.
[65] L. Chai, J. Liu, G. Chen, and X. Zhao, "Dynamics and synchronization of a complex-valued star network," *Sci. China Technol. Sci.*, vol. 3, pp. 1–15, Nov. 2021.
[66] J. Liu, G. Chen, and X. Zhao, "Generalized synchronization and parameters identification of different-dimensional chaotic systems in the complex field," *Fractals*, vol. 29, no. 4, Jun. 2021, Art. no. 2150081.